Nexo Revista Científica
Vol. 36, No. 06, pp. 876-891/Diciembre 2023
ISSN-E 1995-9516
Universidad Nacional de Ingeniería

http://revistas.uni.edu.ni/index.php/Nexo
https://doi.org/10.5377/nexo.v36i06.17443

The Seismic Performance of Infill and Retrofitted Structural Walls under Earthquakes

El comportamiento sísmico de los muros estructurales de relleno y modernizados bajo terremotos

Vafa Morsali*, Farzad Babamohammadi, Jahangir Elyasi

Department of Civil Engineering, Saghez Branch, Islamic Azad University, Saghez, Iran.

*Corresponding author: vafa.morsali@yahoo.com

(recibido/received: 29-agosto-2023; aceptado/accepted: 01-noviembre-2023)

ABSTRACT

To account for the effects of infill walls, the Iranian Code reduces the period of the structure. As a result, filler walls in the plane of structural frames result in significant changes in the properties they possess; therefore, the resistance, stiffness, ductility, distribution of internal forces, and other characteristics of such a frame with an empty frame differ greatly. In this research using 7 far-field earthquakes, a nonlinear time history analysis was performed on reinforced concrete frames with and without masonry infill walls. The maximum relative displacements between the stories were determined. Also, to evaluate the seismic performance of structural masonry walls, the fragility curve of unreinforced masonry walls retrofitted with FRP sheet based on different scenario under the effect of earthquake loads has been investigated by the finite element method. According to the results, the presence of infill walls reduces the number of plastic hinges as well as the maximum relative displacement between the stories. Furthermore, by increasing the number of FRP sheet layers and the reinforced area of the FRP sheet to the entire wall of an unreinforced structural wall, the seismic behaviour of the wall is more effective than other reinforcement patterns and damages the wall less.

Keywords: time history analysis, infill wall, structural wall, plastic hinge, seismic performance.

RESUMEN

Para tener en cuenta los efectos de los muros de relleno, el Código iraní reduce el período de la estructura. Como resultado, los muros de relleno en el plano de los marcos estructurales resultan en cambios significativos en las propiedades que poseen; por lo tanto, la resistencia, rigidez, ductilidad, distribución de fuerzas internas y otras características de dicho marco con un marco vacío difieren mucho. En esta investigación utilizando 7 terremotos de campo lejano, se realizó un análisis histórico no lineal en marcos de hormigón armado con y sin muros de relleno de mampostería. Se determinaron los desplazamientos relativos máximos entre los pisos. Además, para evaluar el comportamiento sísmico de los muros estructurales de mampostería, se investigó mediante el método de elementos finitos la curva de fragilidad de los muros de mampostería no reforzados reequipados con láminas de FRP en diferentes escenarios bajo el efecto de cargas sísmicas. Según los resultados, la presencia de muros de relleno reduce el número de bisagras plásticas, así como el desplazamiento relativo máximo entre los pisos. Además, al aumentar el

número de capas de láminas de FRP y el área reforzada de la lámina de FRP en toda la pared de un muro estructural no reforzado, el comportamiento sísmico del muro es más efectivo que otros patrones de refuerzo y daña menos el muro.

Palabras clave: análisis histórico-temporal, muro de relleno, muro estructural, bisagra plástica, desempeño sísmico

1. INTRODUCCION

To separate the space between the inside and outside of the building, as well as the interior spaces of the buildings, masonry infill walls are used. These are usually placed inside the frame. During an earthquake, this is a critical issue. Although the presence of this wall increases the stiffness of the whole structure, this effect is not always positive. As a result of the increased stiffness of the structure, more earthquake energy is absorbed, but because common masonry wall materials are brittle, they result in early destruction of this member, which is severely reduced the lateral strength of the structure as a result. It is important to consider the effects of infill walls on the structure's frame if they are connected to the frame. As it was indicated, infill walls have different positive and negative impacts on the linear and non-linear behavior of structures. Modeling the various factors that affect structures' responses is extremely time-consuming, difficult, and complicated. However, computers today make it practically impossible to model all of these factors. Researchers have become increasingly interested in calculating and understanding the behavior of structures in the nonlinear domain. Among the methods used in this field, design based on performance has been the most successful; a method that can accurately predict the behavior and performance of structures during severe earthquakes and nonlinear events.

While more than six decades of study have been devoted to modeling methods and the influence of the infill wall on the seismic behavior and performance of structures, there are numerous cases on the subject that require further investigation. This is due to the complexities of the existence of various parameters and the behavioral diversity of materials. There has been widespread failure of masonry infill walls and damage to frames caused by past earthquakes. There were also interactions with the infill walls, twisting in the structure because the infill walls were distributed asymmetrically. This was followed by the collapse of the structures due to the removal of the infill wall which created a soft story. Based on these cases, it appears that there are weaknesses in the design, calculation, and implementation of infill wall building components. In addition, it appears that there is the complexity of their interaction with the main structural components of the building. In 1966, Stafford study the behavior of diagonally-loaded square infilled frames based on frame-infill contact length, in this research methods are adapted to predict lateral stiffness and strength for laterally-loaded infilled frames, supported by experimental results on single and double-story models.. Negro and Colombo (1997) investigated the effects of irregularity created in the frames based on the placement of the infill wall. In a study by Shushtari and Samiei (2003), they examined the seismic behavior of concrete structures with brick infill walls. Based on the results, the height, material, and hardness of infill walls affect seismic behavior. In a study, Kose (2009) investigated the infill wall as one of the effective parameters on the fundamental period of RC buildings. A total of 189 building models were generated using the selected parameters and analyzed using the finite element method in three dimensions. In order to determine the fundamental period of the models, iterative modal analysis was employed due to the nonlinear behavior of the infill walls. According to his research, RC frames with infill walls exhibit a shorter period, about 5% to 10%, compared to RC frames without infill walls. As Razzaghi and Javidnia (2015) demonstrate, neglecting the effects of infill walls during RC frame nonlinear dynamic analysis can dramatically bias the seismic performance of the structure. For this purpose, 18 models of the same structure with different arrangements of infill walls were examined. According to their findings, it is possible to alter the building's damage state during an earthquake by changing the arrangement of infill walls. Peng et al (2018) assess the impact of connection type and structural details of the filler on the cyclic behavior of reinforced concrete (RC) frames using a quasi-static test on four infilled frame samples and one empty frame sample. They concluded that masonry infill walls enhance the lateral strength, stiffness, ductility, and energy

dissipation capacity of the RC frame. A study of full-scale IM walls was carried out by Furtado et al (2016), which included three out-of-plane tests (cyclic and monotonic) with and without previous in-plane damage. It is presented and discussed how the experiments, the material characterization, and the test set-up were performed as well as the results of the test, namely the hysteretic force-displacement curves, the damage evolution, stiffness degradation, and the energy dissipation. Lyu et al (2022) proposed an innovative infill frame system with isolated infill walls layered with highly ductile concrete (HDC) in order to minimize infill-column interaction and improve lateral and deformation resistance of masonry infilled frames. Based on their findings, the isolated infill solution proposed can effectively minimize the interaction between the isolated infill and column. While the damage to the infill wall was minimal, the damage to the columns was almost identical to the damage to the bare frame. Due to the brittle nature of masonry materials, when buildings made of these materials are subjected to lateral forces, after reaching their maximum strength, they suddenly fail and crumble. Due to the imposition of exorbitant financial costs and the inability to stop the operation of the structure for a certain period of time, it is not feasible to demolish existing buildings and replace them with more sturdy structures during an earthquake. Therefore, strengthening these structures is essential to maintain the structure's stability and the safety of residents (Marini et al. 2017, Zampieri et al. 2019, Gioffré et al. 2023). Several methods can be used to reinforce brick masonry walls, including using metal strips as an external strengthening agent (on the surface of the wall) and coating the surface with shotcrete. It is important to note that these methods, while improving the strength and flexibility of masonry walls to some extent, have some disadvantages, which can result in high costs (Ramaglia et al. 2017, Shabdin et al. 2018, Irshidat and shannaq. 2019). Recently, it has been proposed that the use of FRP sheets, in order to prevent these problems, could be a low-cost and more efficient solution to the issue of seismic strengthening. This method has become a suitable replacement for traditional methods. There has been extensive research carried out in this area based on the numerical modelling of these elements used in this field (Papanicolaou et al. 2011, Ghiassi et al. 2012, Xu et al. 2012, Ismail and Ingham. 2012, Bernat et al. 2013, Lin et al. 2016, Maddaloni et al. 2018, Nyarko et al. 2018, Deng et al. 2020). Thus, the purpose of this study is to investigate the effects of masonry infill walls on the seismic performance of reinforced concrete structures The seismic performance of an unreinforced masonry wall retrofitted with composite fibers is evaluated by studying its fragility curves.

2. INFILL WALLS

In order to isolate the interior space from the exterior space of the building, masonry walls are generally erected within the frame, which is an important and practical consideration during an earthquake. It is not always positive to have a wall in place because the increased hardness of the structure causes more force to be absorbed during an earthquake, on the other hand, due to the brittleness of the common masonry wall materials, it may cause this member to be destroyed early. There is a significant reduction in lateral load. Therefore, paying more attention to this issue and analyzing it can facilitate the prediction of the behavior of structures with infill walls.

2.1. Modeling of infill walls using single compression braces

The inplane elastic stiffness of unreinforced building materials should be determined by using a pressure diametric handle equivalent to the width a, according to equation 1 before cracking (Figure 1) (ISREB. No. 360, 2014). The thickness and elasticity coefficient of the pressure handle are the same as the target frame. The width (in centimeters) is:

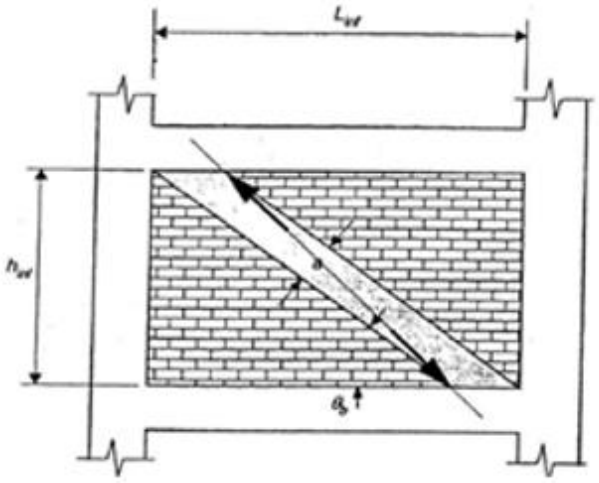

Figure 1. Modeling of infill wall [fema]

$$a = 0.254(\lambda_1 h_{col})^{-0.4} r_{inf} \times R_1 \times R_2, \lambda_1 = \left[\frac{10 E_{me} t_{inf} sin2\theta}{E_{fe} I_{col} h_{inf}}\right]^{0.25} \quad \textbf{(1)}$$

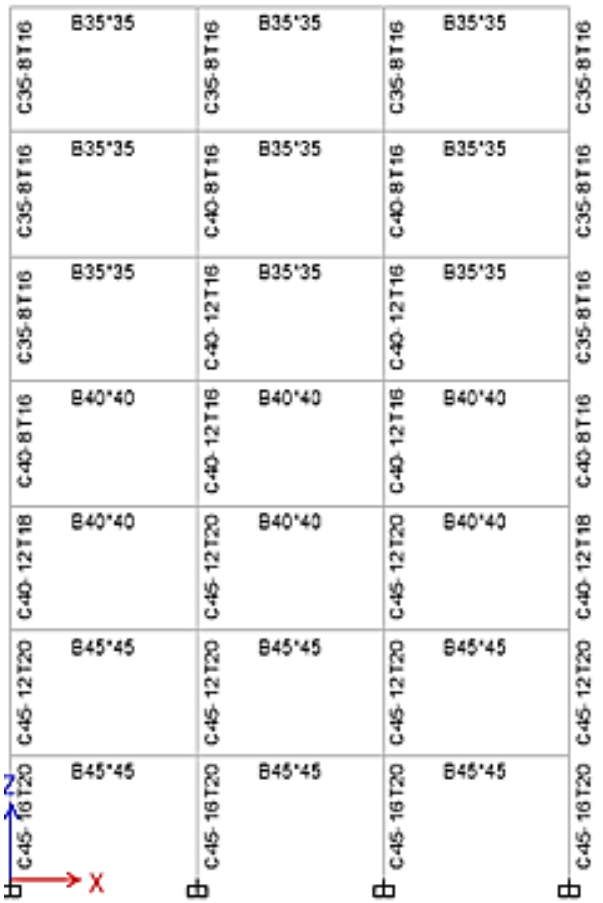

Figure 2. Story Structure

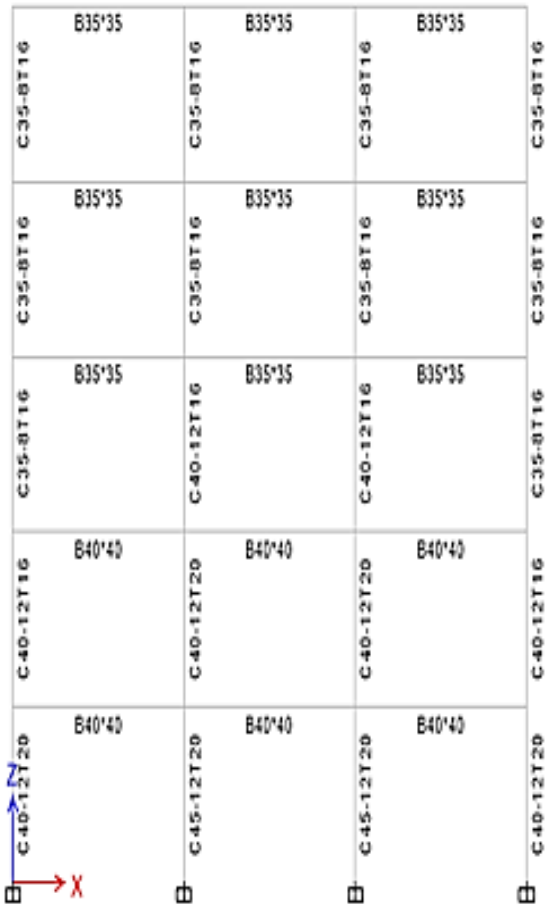

Figure 3. Story Structure

2.2. Numerical examples

The considered structure is the frame of a 5- and 7-story building, regular in plan and height, consisting of a concrete bending frame with medium ductility in both directions of the plan, according to figures 2 and 3 with residential use, located on type 3 soil according to the grouping of the fourth edition of the Iranian seismic code (BHRC-St. No. 2800. 2014). And it is in a region with high seismicity. The spans are 5 meters wide and the stories are 3 meters high. The design of the structure is based on Iranian codes (INBC-part6. 2019, INBC-part 10. 2020). These sections have been loaded, analyzed and designed, and all seismic requirements have been met. For loading the structures, a dead load of 1375 Kgf/m, a live load of 375 Kgf/m, and a roof snow load of 500 Kgf/m have been considered. The specifications for the rebar in the structures are given in tables 1 and 2.

Table 1: The specifications of the concrete used

Compressive resistance	240Kg/cm2
Modulus of elasticity	230000Kg/cm2
Poisson's ratio	0.2

Table 2: The specifications of the steel used

Modulus of elasticity	F_y	F_u
2000000 kg/cm^2	4000 kg/cm^2	6000 kg/cm^2

2.3. Used earthquake records

According to ASCE 7-10 (2016), seven types of ground motions are considered in this paper. Based on data obtained from the University of Berkeley database (PEER), accelerograms were selected. In selecting the accelerograms, a distance from 20 to 70 kilometers was considered for these records as far-fault records. The records have been scaled in this study based on soil type 2 of the Iranian seismic code (BHRC-St. No. 2800. 2014) with shear velocity ranging between 350 and 750 m/s. Accelerograms are scaled based on the wavelet theory, this software is capable of matching earthquake acceleration with a spectrum of target response. The new theory of wavelet has replaced classic theories, such as the Fourier theory, in dealing with different issues in seismology. The specifications of the earthquakes in this study are presented in Table 3. Since the investigated structures are two-dimensional, it is unnecessary to select a pair of mappings, and maximum horizontal components of the above
records have been used for analysis.

Table 3. Earthquakes used in far-fault records

ID	Event Name	Year	Fault distance (km)	Magnitude (Richter)
A	Kern County	1952	38.42	7.36
B	San Fernando	1971	35.54	6.61
C	Coalinga-01	1983	45.49	6.36
D	Morgan Hill	1984	31.88	6.19
E	N. Palm Springs	1986	64.68	6.06
F	Taiwan SMART1(45)	1986	51.35	7.3
G	Loma Prieta	1989	40.85	6.93
A	Landers	1992	69.21	7.28
B	Northridge-01	1994	50.47	6.69
C	Chi-Chi, Taiwan	1999	41.36	7.62

2.5. Calculating the equivalent braces for infill walls

A single compression brace method is used in this article to model the infill wall materials in structural analysis. In order to construct an equivalent brace, it is necessary to determine the compressive strength of the infill wall materials, the modulus of elasticity of the infill wall, and the depth and width of the equivalent brace. Based on different sources, the modulus of elasticity of infill wall materials is estimated to range between 400 and 700 times the compressive stress. According to ISREB. No. 360 (2014), the modulus of elasticity of building materials will be 550 times the compressive stress of infill wall materials. As a result, the following specifications apply:

$$E_{me} = 550 \times f_{me} \quad (2)$$

f_{me} is the compressive stress of the infill wall material, which is equal to 40 kg/cm^2. Then E=22000 kg/cm^2. For all the infill walls of different stories, the diagonal brace width equivalent to an infill wall with a depth of 20 cm can be found in Tables 1 and 2 using (Relation 1). To model the purely compressive performance of these panels, the maximum tensile force of the cross braces is entered as zero, and the cross braces are considered crosswise in the model in order to calculate the cross-sectional area of the compression braces. The specifications of the braces equivalent to the infill walls are given in tables 4 and 5.

Table 4. Specifications of the braces equivalent to the infill walls for 5-story frame

Story	Compressive Strength	Modulus of elasticity	Depth of equivalent brace	Width of equivalent brace
5	40 kg/cm^2	22000 kg/cm^2	20 cm	56 cm
4				59.30 cm
3				59.36 cm
2				59.41 cm
1				62.22 cm

Table 4. Specifications of the braces equivalent to the infill walls for 7-story frame

Story	Compressive Strength	Modulus of elasticity	Depth of equivalent brace	Width of equivalent brace
7	40 kg/cm^2	22000 kg/cm^2	20 cm	57.98 cm
6				57.98 cm
5				57.98 cm
4				60.99 cm
3				61.10 cm
2				63.38 cm
1				64.00 cm

2.6. Non-linear dynamic analysis of models

ETABS software was utilized to perform the nonlinear dynamic analysis of the selected records after the frames and loads had been modelled, defined, and assigned nonlinear behaviours to the elements. The plastic joints in the beams and columns, as well as the maximum relative displacement, were then examined.

2.7. Structural analysis results

Based on the analysis, the distribution of plastic hinges and the relative displacement of the stories have been examined. Tables 5-8 show the state of the plastic hinges in the beams and columns of the 5- and 7-

story structures under selected records. Moreover, Figures 4-7 illustrate the maximum drift ratio of the stories of the 5- and 7-story structures under selected records.

Table 5. Beam hinges distribution of 5- story frame

Earthquake	Infilled	Unfilled	Infilled	Unfilled	Infilled	Unfilled
	IO		LS		CP	
A	10	15	0	0	0	0
B	0	1	0	0	0	0
C	12	15	6	0	0	14
D	7	12	0	5	0	13
E	0	6	0	0	0	5
F	0	2	0	0	0	12
G	15	3	0	0	0	24
Sum	44	54	6	5	0	68

Table 6. Column hinges distribution of 5- story frame

Earthquake	Infilled	Unfilled	Infilled	Unfilled	Infilled	Unfilled
	IO		LS		CP	
A	0	0	0	0	6	4
B	0	0	0	0	0	0
C	13	0	4	0	6	4
D	14	0	0	0	0	2
E	10	0	1	0	0	0
F	14	0	0	0	0	0
G	24	0	0	0	2	4
Sum	75	0	5	0	14	14

Based on the tables above, infill walls have improved the structural performance during all earthquakes. The number of beam hinges was increased only during the C earthquake in the LS range and during the G earthquake in the IO range. During these two earthquakes, however, there were no plastic hinges in the CP range. There has been a slight increase in the number of hinges in columns only in the IO range under C and G earthquakes. The number of hinges has been reduced to zero in the LS and CP ranges. As can be seen from the sum of the hinges in both tables, the presence of an infill wall has significantly enhanced the performance of the columns and beams.

Table 7. Beam hinges distribution of 7- story frame

Earthquake	Infilled	Unfilled	Infilled	Unfilled	Infilled	Unfilled
	IO		LS		CP	
A	0	0	0	0	33	0
B	0	0	0	0	21	0
C	0	0	0	0	36	6
D	0	0	0	0	22	2
E	0	0	0	0	36	0
F	0	0	0	0	36	0
G	0	0	0	0	13	20
Sum	0	0	0	0	197	28

Table 8. Column hinges distribution of 7- story frame

Earthquake	Infilled	Unfilled	Infilled	Unfilled	Infilled	Unfilled
	IO		LS		CP	
A	0	1	0	0	9	0
B	0	0	0	0	0	0
C	0	0	0	0	4	4
D	0	2	0	0	2	2
E	0	1	0	0	8	0
F	0	1	0	0	8	0
G	0	2	0	0	0	2
Sum	0	7	0	0	31	8

Tables 7 and 8 illustrate the condition of the plastic joints created in the beams and columns of the 7-story structure. Due to the presence of an infill wall, the structure performed better in all earthquakes, except in limited cases. These two tables provide the total number of plastic joints created in the beams and columns of the structure for all seven earthquakes. According to these tables, the presence of an infill wall has significantly improved the seismic performance of the columns and the seismic performance of the beams, with the exception of a few areas. It can also be seen that at the base of the columns in frames with infill walls, plastic hinges of the CP type are formed. In addition to strengthening the frames, the presence of the infill wall causes large shear at the base of the columns (resulting in a short column), and this effect must be taken into account when designing the structure.

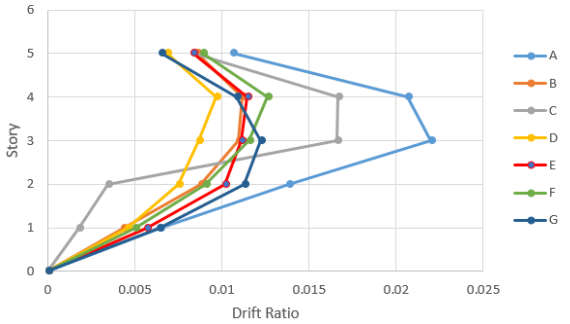

Figure 4. Maximum drift ratio of the stories of the 5-story frame without infill walls

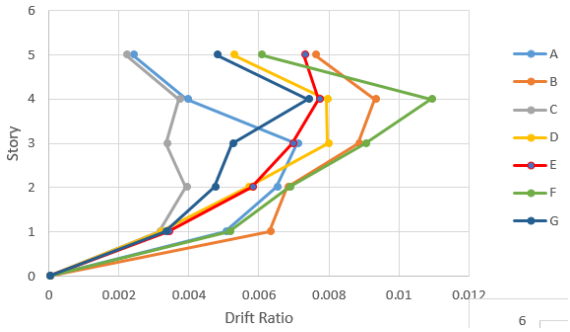

Figure 5. Maximum drift ratio of the stories of the 5-story frame with infill walls

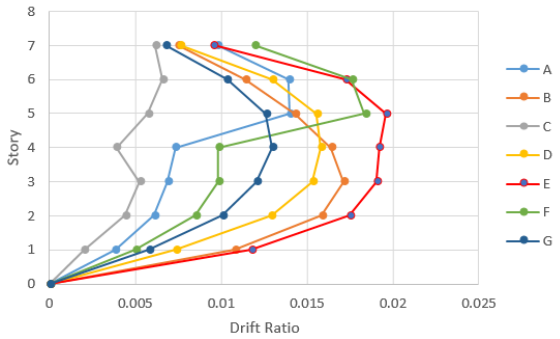

Figure 6. Maximum drift ratio of the stories of the 7-story frame without infill walls

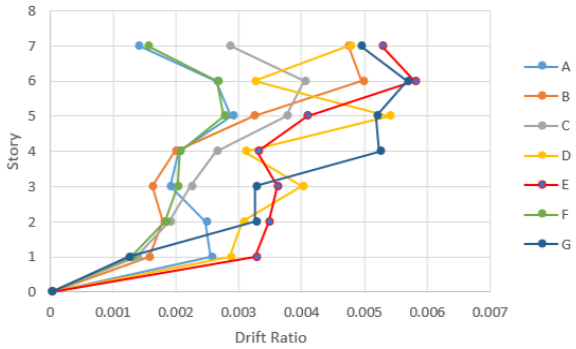

Figure 7. Maximum drift ratio of the stories of the 7-story frame with infill walls

According to Figures 4-8, the strongest effects were observed in the stories of the 5-story building under the A and F earthquakes. As for the 7-story structure, most displacement effects were caused by the E earthquake. As a result of observing the above-mentioned figures, it is also possible to conclude that in structures without infill, other than the first story, other stories experience significant changes in relative displacements. In order to better understand the effects of infill walls, Figures 8-9 present average drift ratios of stories under 7 earthquakes for states with and without infill walls.

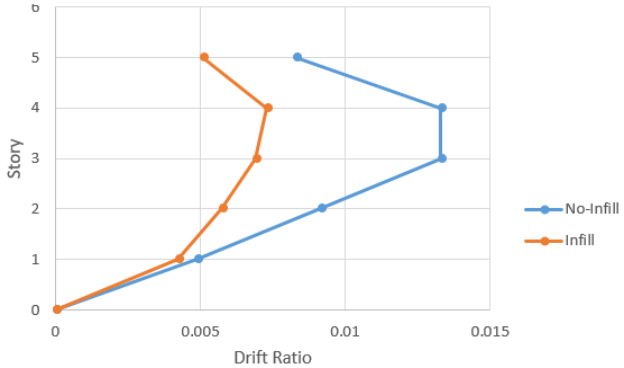

Figure 8. Average drift ratio of the stories of the 5-story frame

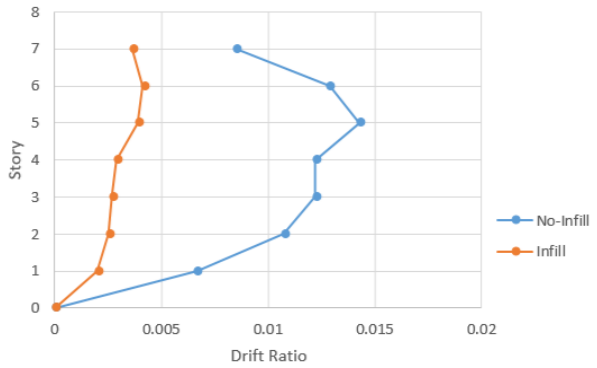

Figure 9. Average drift ratio of the stories of the 7-story frame

As is clear from figures 8-9. The existence of infill walls has effectively reduced the relative displacement of the stories, and as a result, the damage to the stories has been reduced. Because one of the main components of the damage indices is the change in the relative displacement of the stories. Additionally, one of its effects is the uniform distribution of relative displacements on the stories of the studied structures.

3. RETROFITTED STRUCTURAL WALLS

A wall with a length of 180 cm, a height of 120 cm, and a thickness of 22 cm is considered in this section for the purpose of seismic evaluation. The average thickness of mortar in each row is 1 cm. For the equivalent Cohesive, which is equivalent to the mortar of the horizontal and vertical seams, the same properties have been considered. The brick's characteristics and the Cohesive 's characteristics are shown in tables 9 and 10.

Table 9. The brick specifications of

Element	E	V
Brick	1020 N/mm^2	0.15

Table 10. The Cohesive specifications of

Element	Elastic			Damage					
Cohesive	`K_{nn}	k_{ss}	k_{tt}	f_n	f_s	f_t	G_n^I	G_s^{II}	G_t^{III}
	82	36	36	0.027	0.14	0.14	0.03	0.15	0.013

The Drager-Prager's model was used in this research. As well, the C3D8R element with eight nodes and reduced integration was used for modeling the masonry wall, and the S4R element with four nodes was used for modeling the FRP wall. A summary of the models examined in this study is presented in Table 11. Models number 1 and 2 are reinforced horizontally with two CFRP strips. Models 3 and 4 incorporate horizontal reinforcements with three CFRP strips, models 5 and 6 incorporate vertical reinforcement with double CFRP strips, models 7 and 8 incorporate vertical reinforcement with three CFRP strips, and models 9 and 10 incorporate CFRP strips that strengthen the entire wall surface. Table 12 shows the specifications of CFRP sheets.

Table 11. Specifications of examined models

Model	Specimen	L (mm)	H (mm)	T (mm)
1	2H-CFRP-2×3mm	1800	200	6
2	2H-CFRP-4×3mm	1800	200	12
3	3H-CFRP-2×3mm	1800	200	6
4	3H-CFRP-4×3mm	1800	200	12

5	2V-CFRP-2×3mm	1800	200	6
6	2V-CFRP-4×3mm	1800	200	12
7	3V-CFRP-2×3mm	1800	200	6
8	3V-CFRP-4×3mm	1800	200	12
9	ALL-CFRP-2×3mm	1800	1200	6
10	ALL-CFRP-4×3mm	1800	1200	12

Table 12. The Cohesive specifications

Density ($^{kg}/_{m^3}$)	E (GPa)	G (GPa)	V
1600	65.4	5	0.15

3.1. Fragility curves

Fragility curves indicate the probability of damage to a structure at different performance or damage levels. By using the diagrams, researchers will be able to identify and analyze the parameters governing the intensity of each structure's movements. There are four levels of performance examined in these curves: slight damage (drift ratio=0.006), moderate damage (drift ratio=0.012), severe damage (drift ratio=0.03), and completely destroyed (drift ratio=0.08) performance. It is possible to express the level of response of the structure at this performance level by considering different values of stimulus intensity, such as PGD, PGV, and PGA. A fragility curve can be generated using a variety of methods. One of these methods is the analytical method, which is based on the analysis of models. In the analytical method, fragility curves can be drawn by selecting the desired performance level and the number of different earthquake records.

3.1. Dynamic analysis and extraction of fragility curves

In this section, the fragility curves of an unreinforced masonry wall retrofitted with CFRP sheets under seismic loads have been presented and investigated. The stimulation intensity criterion used in these curves is the PGA criterion. Also, the maximum story drift is considered a damage criterion. The damage scale is divided into four levels: minor, moderate, severe and complete damage. In this section, ABAQUS software was used to carry out non-linear analyses. Figures 10 to 22 show the fragility curves of the models described in Table 11.

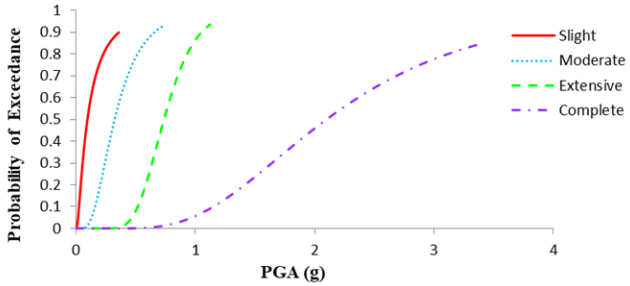

Figure 10. Fragility curve of model number 1

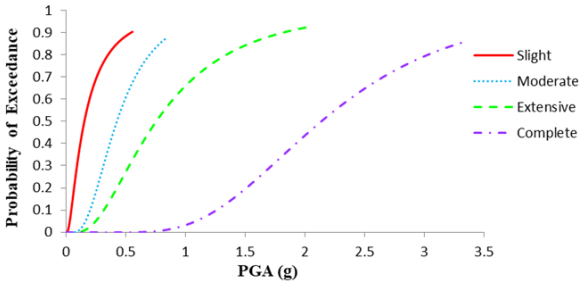

Figure 11. Fragility curve of model number 2

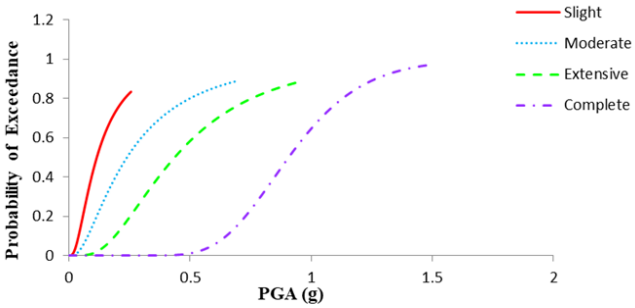

Figure 12. Fragility curve of model number 3

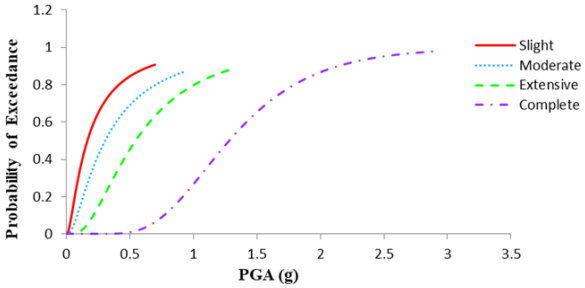

Figure 13. Fragility curve of model number 4

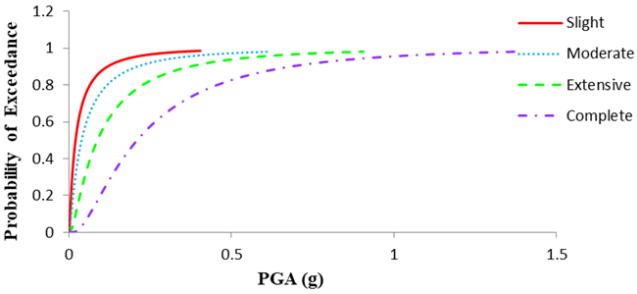

Figure 14. Fragility curve of model number 5

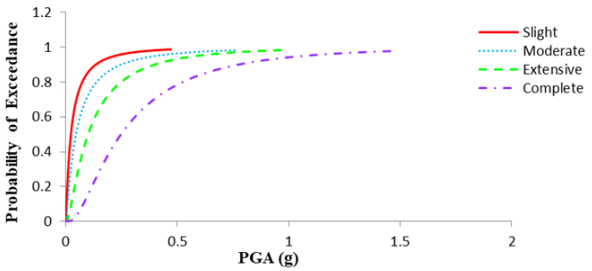

Figure 15. Fragility curve of model number 6

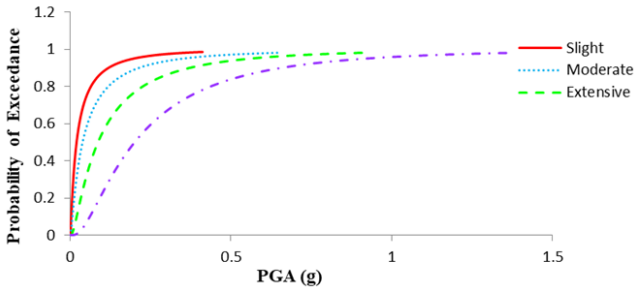

Figure 16. Fragility curve of model number 7

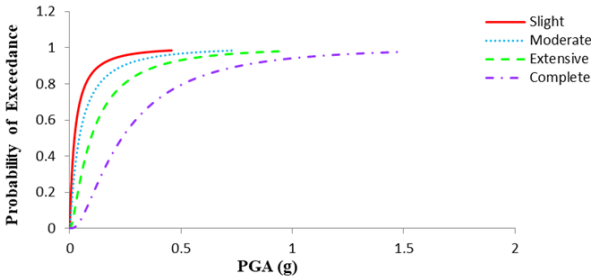

Figure 17. Fragility curve of model number 8

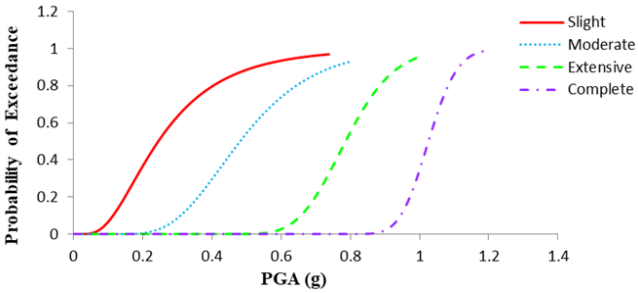

Figure 18. Fragility curve of model number 9

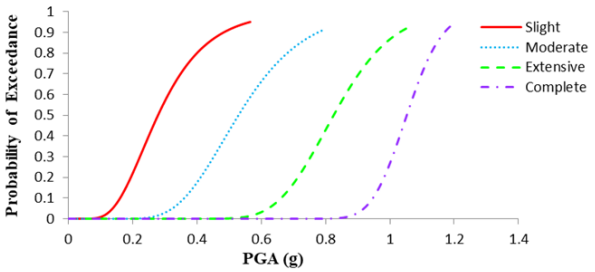

Figure 19. Fragility curve of model number 10

can be seen from figures 10-19 that the more polymer layers there are, the higher the PGA value is, the less damage occurs, and the structure performs better. In addition, horizontally arranged polymer sheets create a better performance in a wall than vertically arranged polymer sheets. It is obvious, in this case, that there is a greater probability of passing a performance criterion for lower PGAs. Also, in order to compare structural damage levels quantitatively, Table 33 provides PGA values for each level corresponding to different models.

Table 13. PGAs corresponding to structural damage levels (g)

Models	Slight	Moderate	Extensive	Complete
1	0.31	0.67	1.04	3.35
2	0.29	0.65	1.03	3.33
3	0.23	0.66	0.9	1.46
4	0.6	0.64	1.19	2.82
5	0.39	0.6	0.86	1.34
6	0.38	0.7	0.92	1.43
7	0.38	0.59	0.85	1.36
8	0.43	0.71	0.92	1.46
9	0.51	0.77	0.97	1.16
10	0.53	0.76	0.96	1.14

Based on Table 13, it can be seen that for a certain probability of passing, models 1 and 2 have the potential to experience more PGAs. In other words, the probability of failure in them increases greatly.

4. CONCLUSIONS

This study investigated The seismic performance of infill and retrofitted structural walls under earthquakes. In light of the fact that plastic hinge deformation is used in determining the extent of damage to beams, columns, and the structure as a whole, it is possible to conclude that the reduction of plastic joints in areas beyond life safety can be considered a method of damage control in structures. It can be seen from the tables and figures that the presence of infill walls in the structure has reduced the number of plastic hinges, especially in areas beyond life safety, and, on the other hand, the relative displacement of the stories has also decreased. By comparing the results, it can be concluded that the infill wall has reduced the damage mainly in the beams, as well as the drift ratio of the stories. Generally, it can be concluded that the infill wall in the structure can be a damage control factor as well as a control factor for the change of relative displacements of the stories. It was also found that the arrangement and number of CFRP layers can create different fragility curves for reinforced structural walls. In addition, the level of vulnerability depends on the number and arrangement of CFRP layers. In comparison with the other models, models 6 and 7 as well as models 9 and 10 performed better. As a result, within the 10 reinforced models, model 10 was the model that performed the most effectively in terms of seismic performance.

5. REFERENCES

American Society of Civil Engineers (ASCE). 2016. Seismic Evaluation and Retrofit of Existing Buildings. Reston, Virginia.

Bernat, E., Gil, L., Roca, P., & Escrig, C. 2013. Experimental and analytical study of TRM strengthened brickwork walls under eccentric compressive loading. Construction and Building Materials, 44, 35-47. Earthquake Engineering, Lisbon, Portugal (pp. 24-28).

Building and Housing Research Center (BHRC). (2014). “Iranian code of practice for seismic resistant design of buildings", Iranian National Seismic Code (Standard. No. 2800), Tehran, Iran.

Deng, M., Zhang, W., & Yang, S. 2020. In-plane seismic behavior of autoclaved aerated concrete block masonry walls retrofitted with high ductile fiber-reinforced concrete. Engineering Structures, 219, 110854.

Furtado, A.,Rodrigues, H., Arêde, A., Varum,H. 2016. Experimental evaluation of out-of-plane capacity of masonry infill walls. Engineering Structures, Vol 111, PP 48-63.

Ghiassi, B., Soltani, M., & Tasnimi, A. A. 2012. Seismic evaluation of masonry structures strengthened with reinforced concrete layers.

Gioffré, M., Navarra, G., Cavalagli, N., Iacono, F. L., Gusella, V., & Pepi, C. 2023. Effect of hemp bio composite strengthening on masonry barrel vaults damage. Construction and Building Materials, 367, 130100.

Instruction for Seismic Rehabilitation of Existing Buildings (ISREB. No. 360). 2014. Management and Planning Organization of Iran, Iran.

Irshidat, M. R., & Al-Shannaq, A. 2019. Bond strength evaluation between textiles reinforced mortar with carbon nanotubes and concrete substrate. Latin American Journal of Solids and Structures, 16.

Ismail, N., & Ingham, J. M. 2012. In-situ and laboratory based out-of-plane testing of unreinforced clay brick masonry walls strengthened using near surface mounted twisted steel bars. Construction and Building Materials, 36, 119-128.

Kose, MM. 2009. Parameters affecting the fundamental period of RC buildings with infill walls. Engineering Structures, Volume 31, Issue 1, Pages 93-102.

Lin, Y., Lawley, D., Wotherspoon, L., & Ingham, J. M. (2016). Out-of-plane testing of unreinforced masonry walls strengthened using ECC shotcrete. In Structures (Vol. 7, pp. 33-42). Elsevier.

Lyu, H., Deng, M., Han, Y., Ma, F., Zhang, Y. 2022. In-plane cyclic testing of full-scale reinforced concrete frames with innovative isolated infill walls strengthened by highly ductile concrete. Journal of Building Engineering, Vol 111, 104934.

Maddaloni, G., Di Ludovico, M., Balsamo, A., Maddaloni, G., & Prota, A. 2018. Dynamic assessment of innovative retrofit techniques for masonry buildings. Composites Part B: Engineering, 147, 147-161.

Marini, A., Belleri, A., Preti, M., Riva, P., & Giuriani, E. 2017. Lightweight extrados restraining elements for the anti-seismic retrofit of single leaf vaults. Engineering Structures, 141, 543-554.

Ministry of Housing and Urban Development (INBC). 2019. Iranian National Building Code for Structural Loadings-Part 6. Tehran, Iran.

Ministry of Housing and Urban Development (INBC). 2020. Iranian National Building Code for Concrete Structures -Part 10. Tehran, Iran.

Negro P, Colombo A. 1997. Irregularities induced by nonstructural masonry panels in framed buildings, Engineering Structures. Vol, 19, PP: 576-585.

Nyarko, H. M., Ademovic, N., Pavic, G., & Sipos, T. K. 2018. Strengthening techniques for masonry structures of cultural heritage according to recent Croatian provisions. Earthquakes and Structures, 15(5), 473-485.

Papanicolaou, C., Triantafillou, T., & Lekka, M. 2011. Externally bonded grids as strengthening and seismic retrofitting materials of masonry panels. Construction and Building Materials, 25(2), 504-514.

PEER: NGA Database, Pacific Earthquake Engineering Research Center, University of California, Berkeley, http://peer.berkeley.edu/nga/.

Quanmin, P., Xiaojie, Zh., Chenghao, Y. 2018. Influence of connection and constructional details on masonry-infilled RC frames under cyclic loading. Soil Dynamics and Earthquake Engineering, Vol 108, PP 96-110.

Ramaglia, G., Lignola, G. P., Balsamo, A., Prota, A., & Manfredi, G. (2017). Seismic strengthening of masonry vaults with abutments using textile-reinforced mortar. Journal of Composites for Construction, 21(2), 04016079.

Razzaghi, M. S., Javidnia, M. 2015. Evaluation of the effect of infill walls on seismic performance of RC dual frames. International Journal of Advanced Structural Engineering (IJASE), Volume 7, Issue 1, Pages 49-54.

Shabdin, M., Zargaran, M., & Attari, N. K. 2018. Experimental diagonal tension (shear) test of Un-Reinforced Masonry (URM) walls strengthened with textile reinforced mortar (TRM). Construction and building materials, 164, 704-715.

Stafford, B. S. 1966. Behavior of square infilled frames. Journal of the Structural Division. Vol 92, PP: 381-403.

Xu, L. H., Zhang, S., Hu, X. B., & Zhang, M. J. (2012,). Seismic responses of masonry structures strengthened with FRP laminates: A shaking-table study. In Proceedings of the 15th World Conference on Earthquake Engineering.

Zampieri, P., Gonzalez-Libreros, J., Simoncello, N., & Pellegrino, C. (2019). Strengthening of masonry arches with frcm composites: A review. Key Engineering Materials, 817, 251-258.